DOI: 10.1002/mds3.10144

RESEARCH ARTICLE

MEDICAL DEVICES & SENSORS WILEY

Next-generation Antimicrobial Peptides (AMPs) incorporated nanofibre wound dressings

Ayda Afshar[1] | Esra Yuca[2] | Cate Wisdom[2,3] | Hussain Alenezi[1,4] | Jubair Ahmed[1] | Candan Tamerler[2,3] | Mohan Edirisinghe[1]

[1]Department of Mechanical Engineering, University College London, London, UK

[2]Institute for Bioengineering Research, University of Kansas (KU, Lawrence, KS, USA

[3]Department of Mechanical Engineering and Bioengineering Program, University of Kansas (KU, Lawrence, KS, USA

[4]Department of Manufacturing Engineering, College of Technological Studies, PAAT, Kuwait City, Kuwait

Correspondence
Mohan Edirisinghe, Department of Mechanical Engineering, University College London, London WC1E 7JE, UK.
Email: m.edirisinghe@ucl.ac.uk

Abstract

Antimicrobial peptides (AMPs) containing polymer-based nanodelivery systems offer to overcome many challenges in wound care. While preventing the contact of the external agents on the wound, it also addresses a rising concern on the drug resistance. AMPs as the host defence peptides have been increasingly recognized for therapeutic potential owning to their critical role in innate immunity. Here we investigated a nanofibre mesh approach using AMPs incorporated polyethylene oxide (PEO) for wound healing applications. PEO was prepared to carry GH12-COOH-M2 (type 1 AMP) and AMP2 (type 2 AMP), and their antibacterial activity was assessed against *Staphylococcus epidermidis (S. epidermidis)*. PEO-AMP nanofibre meshes were successfully formed by using pressurized gyration (PG), which allows rapid mass production. Bacterial viability of the nanofibre meshes was investigated using the AlamarBlue assay. Fibre morphology, size distribution and AMP incorporation in the nanofibres were characterized by scanning electron microscopy (SEM), fluorescence microscopy (polarization contrast images) and Fourier transform infrared spectroscopy (FTIR). While both PEO-AMP1 and PEO-AMP2 nanofibres indicate promising bacterial inhibition at 105 μg/ml, PEO-AMP2 fibres showed the highest *S. epidermidis* reduction. The results demonstrated that increase in the AMP content reduced the bacterial growth. Another important implementation of the PEO-AMP nanofibres is that they can be tuned to rapidly releasing the peptides. Antimicrobial peptide-loaded nanofibres represent a viable biologically active solution to next-generation wound dressings.

KEYWORDS
antimicrobial peptides, fibre, pressurized gyration, staphylococcus epidermidis, wound healing

1 | INTRODUCTION

The skin is the most exposed organ and, therefore, vulnerable to injury and wounds (Nguyen & Soulika, 2019). Wound healing is a complex tissue repair process, and failing to manage it could result in the formation of scars (Landén et al., 2016; Takeo et al., 2015). Tissue repair involves the partial tissue regeneration involving restitution of tissue components during the wound healing process (Atkin et al., 2019; Gonzalez et al.., 2016). Wound healing is a dynamic process consisting of four phases: inflammation, proliferation,

and remodelling (Eming et al., 2014; Ghomi et al., 2019). All four phases should occur in proper sequence in an ideal healing process, as interruptions can result in delayed wound healing and failure to return to the native aesthetic and functional form (Dreifke et al., 2015). The ideal wound dressing should be non-toxic (Jalili Tabaii & Emtiazi, 2018), non-allergic (Negut et al., 2018), promote absorption of wound exudates (Dumville et al., 2016), provide a gaseous exchange, protect against bacterial infection (Dabiri et al., 2016), be easy to apply and remove (Uzun, 2018), and allow for adequate hydration (Hasatsri et al., 2018). Current wound dressing methods such as hydrogels (Kamoun et al., 2017) can maintain a moist wound environment but are not ideal for very wet wounds (Caló & Khutoryanskiy, 2015) where it can lead to infection due to excess moisture (Pilehvar-Soltanahmadi et al., 2017). Hydrocolloidal wound dressings have been successful against bacteria but the dressing may adhere and displace the wound and cause trauma upon removal (Miguel et al., 2019). Thus, a new generation of wound dressing materials (Sood et al., 2014) is expected to control higher moisture levels, and provide sustained release of biologically active ingredients (Georgescu et al., 2017), which will enhance the healing of wounds (Gizaw et al., 2018).

Fibres in the nanometre range are an excellent class of materials for different applications (Lee et al., 2015), including biomaterials (Shahriar et al., 2019) for tissue engineering (Adam et al., 2013; Ye et al., 2019), drug delivery (Al-Enizi et al., 2018), air and water filtration systems (Chen et al., 2019), and wound healing (Liu et al., 2019). Nanofibres can be functionalized into wound dressings due to their distinctive properties; such as a high surface area to volume ratio (Sun et al., 2019) and high porosity that allows for both the protection of the wound site and exudate movement (Han & Ceilley, 2017), which is crucial for optimal recovery (Mir et al., 2018). For increased antibacterial resistance, for settings such as hospitals wound treatment is required that can address issues related to the currently available dressings (Illangakoon et al., 2017). Fibre manufacturing processes such as electrospinning (Xue et al., 2019), centrifugal spinning (Leng et al., 2019) and pressurized gyration (PG) (Heseltine et al., 2018) are able to produce nanofibres. However, among all the approaches, pressurized gyration was selected in this work because of its ability to mass-produce-bandage-like meshes with simple preparation and enhanced processing controls (Alenezi et al., 2019).

Nanofibres loaded with antimicrobial agents such as antibiotics (Thakkar & Misra, 2017), graphene (Lasocka et al., 2019; Matharu et al., 2018), nanoparticles (Hassiba et al., 2017; Troncoso & Torres, 2020) and natural antimicrobial substances (Simoes et al., 2018) are a valuable way to target bacterial species by reducing wound infections (Stone et al., 2018) potentially enhancing the healing process. Nanofibres can release antimicrobial agents with greater efficacy due to their large surface area (Kenry, 2017; Nguyen et al., 2013). The goal is to improve the healing process which would speed up regeneration (Saghazadeh et al., 2018) and reduce scarring (Rahimnejad et al., 2017) by incorporating novel antimicrobial agents into nanofibrous materials. Nanofibres are also able to imitate the extracellular matrix (ECM) (Jun et al., 2018) to provide a suitable cellular niche to accelerate wound repair (Rezk et al., 2018).

Antimicrobial peptides are short generally cationic peptides (Chou et al., 2019) with an amphipathic structure (Agarwal et al., 2016) that are active against certain bacteria, fungi and viruses (Ebenhan et al., 2014; Mahlapuu et al., 2016). The mechanism of antibacterial action is related to their ability to adjust membrane permeability, which destructs the membrane structure of the pathogen. One particular property that makes AMPs effective towards multidrug-resistant bacteria strains (Yang et al., 2019) is in its wide-scale multitargeted action (Joo et al., 2016; Zharkova et al., 2019). Usually, AMPs exhibit a net positive charge with a high ratio of hydrophobic amino acids that allows peptides to selectively bind to negatively charged bacterial membranes (Lei et al., 2019; Zhen et al., 2019) to either disrupt the membrane (Kumar et al., 2018), or to enter the bacterium and inhibit intracellular functions (Yazici et al., 2016). Peptides have low toxicity (Yin et al., 2017), high specificity (Lombardi et al., 2019), and are readily synthesized or modified (Tesauro et al., 2019). GH12 is one of the well-established antimicrobial peptides (Y. Wang et al., 2019). Previously, we have engineered a derivative of GH12, GH12-M2 (GLLWHLLHHLLH_GSGGG_K) and showed its antimicrobial activity (Xie et al., 2019). We have also shown that computationally designed AMP2 (KWKRWWWWR) prevents *S. epidermidis* growth at a very low concentration (Fjell et al., 2011; Yucesoy et al., 2015). AMPs are compatible with the mechanical, functional and structural properties of most polymers and are extremely biocompatible and biodegradable (Sharma et al., 2015). Nanofibres provide a viable means of delivery for AMPs while providing excellent structural features.

In this study, we investigate the viability of PEO-AMP nanofibres to represent an ideal release system to deliver AMPs for wound healing applications. We designed and produced M2 (type 1 AMP), and AMP2 (type 2 AMP) and integrated PEO nanofibres to make wound dressings. A wound dressing material can be created by loading peptides into water-soluble polymers that are efficient in their release. Such materials at the wound site can provide protection while also releasing active antimicrobial support. Thus, the growth of microorganisms is regulated by the antibacterial agents embedded in the structure of the fibre (Morais et al., 2016). We obtained promising results for both of PEO-M2 (type 1 AMP) and PEO-AMP2 (type 2 AMP) nanofibres on *S. epidermidis*, which will be an effective release mechanism for wound healing applications.

2 | MATERIALS AND METHODS

2.1 | Materials

Polyethylene oxide (PEO, M_w 200,000 $gmol^{-1}$) was purchased from Sigma-Aldrich (Poole, UK). Two AMPs were used including GH12-COOH-M2 (M_w 1932 Da) (type 1 AMP) and AMP2 (M_w 1517.8 Da) (type 2 AMP) and were synthesized at the Tamerler Laboratory at

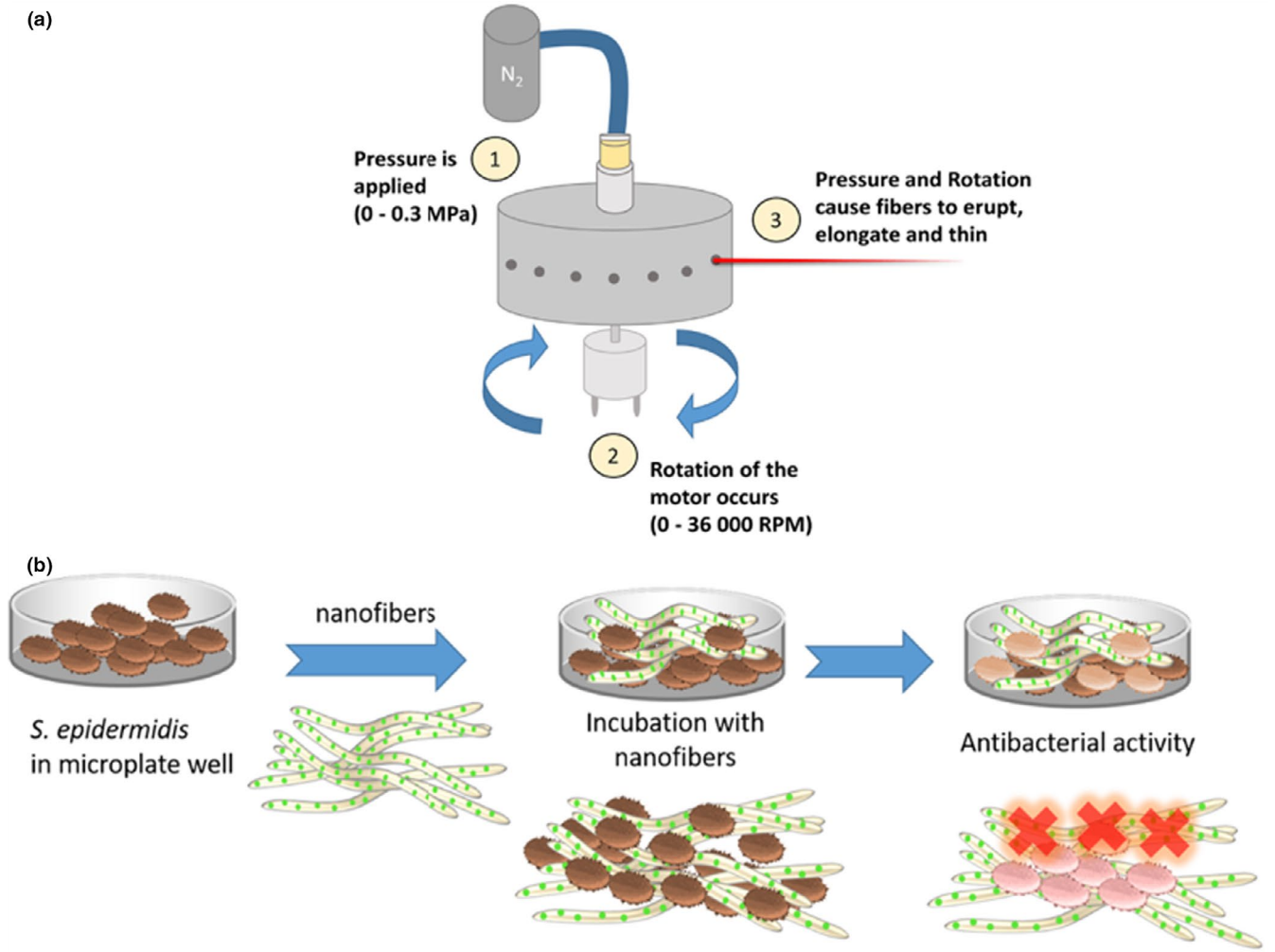

FIGURE 1 (a) Schematic diagram illustrating the pressurized gyration set-up and three key phases leading to fibre production; (b) schematic illustration of the antibacterial assessment protocol for AMP integrated PEO nanofibres

University of Kansas, USA (section 2.2). Distilled water was used as the solvent for all of the polymer solutions in this study.

2.2 | Antimicrobial peptide synthesis and purification

GH12-M2 (M2) (type 1 AMP) and AMP2 (type 2 AMP) AMPs were synthesized by solid-phase peptide synthesis (SPPS) using an AAPPTec Focus XC benchtop peptide synthesizer. Fmoc-rink amide resin with a 0.56 mmol/g substitution factor was used for both peptides. The resin was deprotected by extracting the Fmoc group from dimethylformamide (DMF) with a standard 20% piperidine deprotection solution. UV-absorbance monitored the removal of Fmoc, and DMF was used to wash the deprotected resin to remove piperidine. Modified amino acids with Fmoc and protected sidechains were solubilized in DMF at a concentration of 0.2 M and added to the resins with 7-fold excess of the substitution factor. The solubilized amino acids were activated in a separate measuring vessel in a solution of 0.4 M O-benzotriazole-N, N, N', N'-tetramethyl-uronium-hexafluoro-phosphate (HBTU) in DMF and 1 M 4-methylmorpholine (NMM). The activated amino acids were applied to the deprotected resin and mechanically mixed under nitrogen gas for 45 min to couple the amino acids to the resin. The resin was washed with DMF after the addition of amino acid, and the protocol was repeated for each subsequent amino acid. The resins with synthesized peptides were then dried with ethanol following synthesis to extract residual DMF. The peptides were cleaved from the resin, and the sidechains were deprotected using Reagent K (TFA/ thioanisole/ H2O/ phenol/ ethanedithiol (87.5:5:5:2.5)) and precipitated by cold ether. RP-HPLC was used to purify crude peptides, which were then lyophilized and stored at −20°C.

2.3 | Preparation of polymer and peptide solutions

PEO was prepared at different concentrations, and from preliminary testing, it was found that 15 w/v% produced maximal fibre yield. The following peptide concentrations: 35, 70, 105, 140 and 175 μg/ml, were added to the PEO polymer solutions. The solutions were

magnetically stirred to obtain a homogenous solution and stored at 4°C for 48 h. 15 w/v% PEO solution which was used as a negative control was also prepared and magnetically stirred for 24 h.

2.4 | Pressurized gyration

The PG set-up shown in Figure 1a was used to spin the fibres in this study. The set-up consists of an aluminium cylindrical vessel (60 mm diameter, 35 mm height) with a total of 24 orifices on the wall of the vessel, each opening is 0.5 mm in diameter. The bottom is connected to a DC motor that generates a rotational speed of up to 36,000 rpm, and the top is connected to a constant nitrogen gas stream (N_2) that generates a flow pressure between 0.1 – 0.3 MPa. Before spinning, the polymer solution is poured on the inside of the rotating device. Solvent selection can greatly influence the morphology of the fibres.

High speed and flow pressure cause the polymer solution to erupt as a jet which elongates and thins. As the fibres thin, the solvent evaporates which results in solid fibre formation. In this study, a water-soluble polymer was used as water has a low volatility which allows the solution to elongate for longer, creating thinner strands than what would otherwise have been produced by using more volatile solvents. Furthermore, water has complete biocompatibility *in vivo* and for wound healing applications. In this work, the maximum rotation speed routinely available at the present time was used as it increases the centrifugal force, and as such, forcing the liquid out the perforations with a greater kinetic energy, which results in thinner fibres. When increasing the pressure, fibres with a smaller diameter are generated due to the gas pressure providing better elongation conditions. Finer diameter fibres are more desirable in this research as they correspond to a more intense antimicrobial release ability largely due to an increased porosity and higher available surface area.

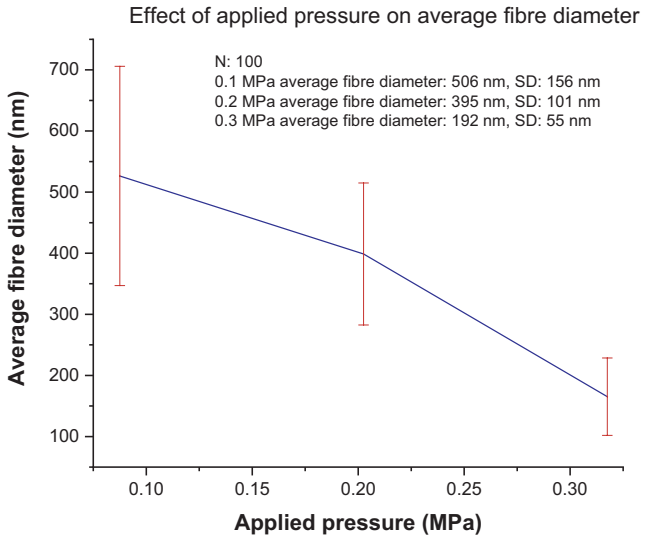

FIGURE 2 Graph showing the effect of applied gas pressure on the fibre diameters using M2 peptides (type 1 AMP) and PEO at low concentrations (35 μg/ml)

2.5 | Fibre characterization

The fibre morphology was analysed using a Hitachi HN004 (Hitachi, Japan) SEM, that operated at an accelerating voltage of 5 kV. The samples were gold sputter coated using Quorum Q1500R ES (Quorum Technologies Ltd., UK) for 90 s before being loading on to the microscope stage. From the digital micrographs, the average fibre diameters were calculated using ImageJ software. In this case, 100 fibre strands were measured at random, and the average was estimated and plotted on histograms using Origin Pro computer software.

2.6 | Fluorescence and polarization imaging

Polarization contrast images were captured on a Zeiss Axioplan2 (Zeiss, Germany) microscope, with a 20×NA0.5 objective. Images were captured as brightfield, or polarization contrast with a pair of crossed polarizers, and two-quarter waveplate circular polarizers at 45 degrees. Images were captured with a Zeiss Axiocam HRc (Zeiss, Germany). Birefringence occurs when polarized light passes through an anisotropic crystalline lattice.

2.7 | Fourier transform infrared spectroscopy (FTIR)

The infrared spectra of nanofibre samples were recorded on a Fourier transform infrared spectroscopy (FTIR) spectrometer (PerkinElmer Spectrum-400, UK) between 4000 and 450 cm^{-1} with a resolution of 4 cm^{-1}.

2.8 | Peptide *de novo* structure modelling

Secondary structure models were developed using the PEP-FOLD 3.5 online server (Lamiable et al., 2016; Shen et al., 2014). PEP-FOLD 3.5 generates 3D structural peptide conformations between 5–50 amino acids long and creates PDB models for the best five structures. The AMP sequences were input, and 200 simulations were performed, assuming aqueous conditions and at a neutral pH. The models were grouped and categorized using sOPEP (optimized potential for efficient structure prediction). The most likely model was imported to UCSF chimera for visualization and recolouring.

2.9 | Antimicrobial activity

Staphylococcus epidermidis (ATCC 2988) was cultured according to the ATCC protocol in Nutrient broth (NB). Rehydrated frozen stock

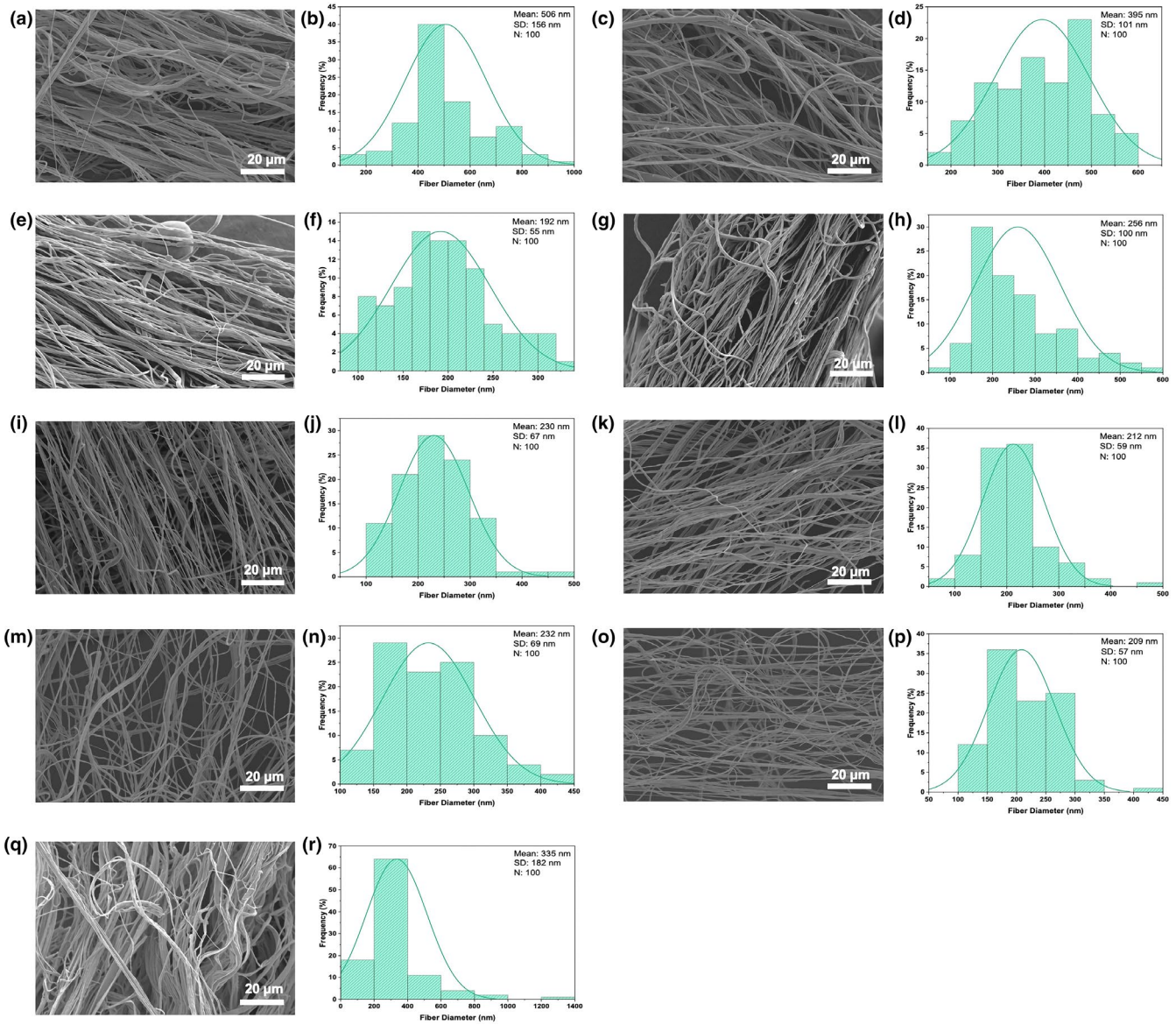

FIGURE 3 SEM images and size distribution graphs of 15 w/v% PEO-water fibres incorporated with: (a,b) type 1 AMP 35 μg/ml (0.1 MPa), (c,d) 35 μg/ml (0.2 MPa), (e,f) 35 μg/ml (0.3 MPa), (g,h) 70 μg/ml (0.3 MPa), (i,j) 105 μg/ml (0.3 MPa), (k,l) 140 μg/ml (0.3 MPa), (m,n) using type 2 AMP 105 μg/ml (0.3 MPa), (o,p) 140 μg/ml (0.3 MPa), (q,r) 15 w/v% PEO-water control (0.3 MPa). The produced fibres were spun at 36,000 rpm

of bacteria was streaked on an NB agar plate and incubated for 24 h at 37°C. A single colony was removed from the agar plate and used to inoculate 5 ml of appropriate medium followed by incubation overnight. Bacteria were grown to mid-log phase with a final concentration of 105 CFU/ml. In-solution antimicrobial activity of the peptide incorporated fibre samples was assessed in 96 well plates. For antimicrobial activity assay, each fibre sample (1 mg) was soaked in 100 μL NB. Fibre containing media were mixed with *S. epidermidis* culture. *S. epidermidis* bacteria without any fibre sample served as the negative control. The 96-well plate was incubated at 37°C overnight. The viability of *S. epidermidis* was measured using an AlamarBlue (Thermo Fisher Scientific) assay. Cellular activity was measured via fluorescence (Ex/Em 565/595 nm) following the bacterial metabolic conversion of resazurin to the fluorescent molecule, resorufin (Figure 1b).

3 | RESULTS AND DISCUSSION

3.1 | Spinning fibres

The PEO-AMP and PEO-control solutions were spun at 36,000 rpm using the PG apparatus. During initial testing, nanofibres were generated using a concentration of 35 μg/ml PEO-M2 (type 1 AMP) at different applied pressures (0.1, 0.2 and 0.3 MPa) (Figure 2) to evaluate the influence of varying pressure on the fibre morphology. The nanofibres were analysed using SEM. It was observed at the lowest applied pressure (0.1 MPa) that the nanofibres had an average fibre diameter of 506 nm ± 155 nm, however by increasing the pressure to 0.3 MPa, the average fibre diameter decreased to 191 nm ± 55 nm. The standard deviation (SD) values are obtained from the fibre

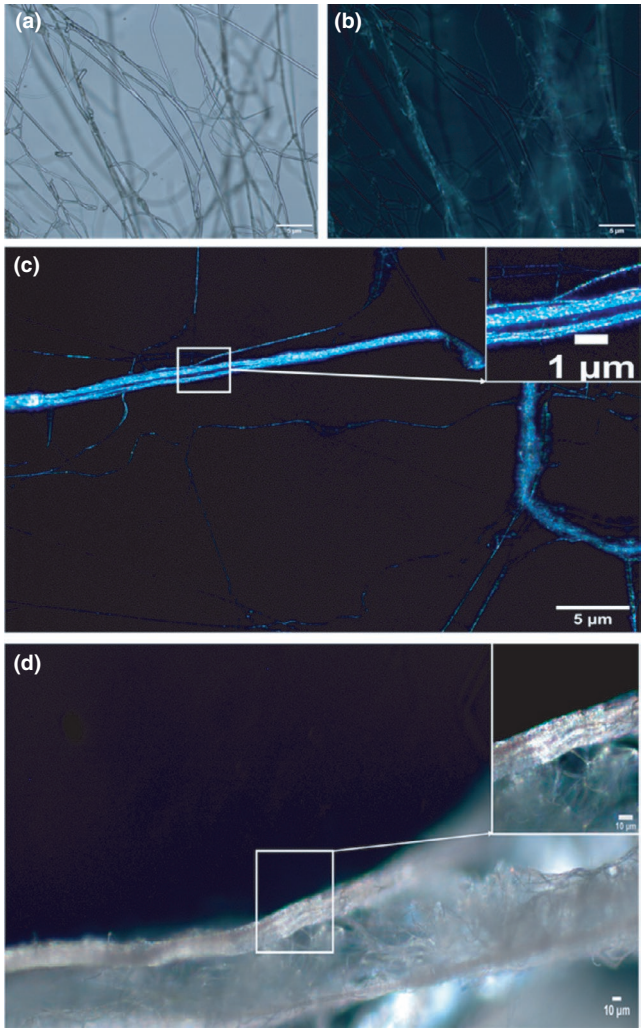

FIGURE 4 Polarization contrast images captured on a Zeiss Axioplan2 microscope, with a 20xNA0.5 objective, (a) Pure PEO fibres without polarization contrast, (b) Pure PEO fibres with polarization contrast, (c) PEO-M2 fibres (type 1 AMP) fibre, and (d) PEO-AMP2 fibres (type 2 AMP) (+ve) polarization image

diameter statistics in Figure 3. Increase in the gas pressure dramatically affects the fibre diameter, forming thinner fibres. Furthermore, at no additional applied pressure, it is considered only centrifugal spinning, and PEO nanofibres were not formed, justifying the requirement for PG. An increase in the AMP content to 70 µg/ml generated an average fibre diameter of 256 nm ± 100 nm. The small fibre diameters achieved highlights that the fibres have a very high surface area to volume ratio and are in the same range as typically observed in the ECM and will be highly beneficial as a wound bandage material (DeFrates et al., 2018).

3.2 | Fibre characterization

The SEM images depict the formed fibres as fine fibre strands with a smooth surface topography (Figure 3). It is emphasized that there is a decrease in fibre size distribution as a result of an increase in the AMP concentration, where uniformity is a highly desired characteristic in wound healing applications.

The average fibre diameter for (M2) peptides at 75 µg/ml is 256 nm ± 100 nm (Figure 3g,h); however by increasing the AMP concentration to 105 µg/ml, the average fibre diameter is reduced to 230 nm ± 67 nm (Figure 3i,j). Further increasing the AMP concentration to 140 µg/ml, the average fibre diameter decreased to 212 nm ± 59 nm (Figure 3k,l). Moreover, using a different peptide, (AMP2), similar effects on nanofibre size distribution were observed. At 105 µg/ml to 140 µg/ml (AMP2), the average fibre diameter decreases from 232 nm ± 69 nm (Figure 3m,n) to 209 nm ±57 nm (Figure 3o,p), respectively. In the case of PEO nanofibres with no AMP, the average fibre diameter at 0.3 MPa was 335 nm ±182 nm (Figure 3q,r). Therefore, it is established that by increasing the AMP concentration in PEO nanofibres, the average fibre diameter decreases and results in a higher surface area to volume ratio.

3.3 | Fluorescence and polarization image analysis

Fluorescent microscopy composed of brightfield microscopy (Figure 4a) followed by polarization contrast (Figure 4b) was performed to compare the appearance of the PEO-control sample and the PEO-AMP nanofibre samples. Brightfield microscopy displayed a clear image with no peptide attachment of the PEO fibre surface (Figure 4a); therefore, polarization contrast images were used to uncover further information. Both images were consistent in suggesting that the PEO-control nanofibres were present with no peptide attachment. To evaluate the appearance of PEO-AMP nanofibres, we used two levels of integration of the PEO samples combined with both M2 (type 1 AMP) and AMP2 (type 2 AMP) AMPs.

Polarization images provided a distinctive representation in the appearance of peptides dispersed on and within the PEO-nanofibre surface. Figure 4c,d indicates the incorporation of type 1 and type 2 AMPs at 105 µg/ml in the fibres. The contrast images confirm the presence of the M2 and AMP2 peptides distributed evenly along the nanofibre surface, illustrated as dots. Figure 4c shows the M2 (type 1 AMP) fibres with peptides on the surface of the 5 µm scale. When adjusting the image to a 1 µm scale, it is obvious that the peptides appear on the surface by the dotted texture. In Figure 4d, the peptides are fused on the surface of the AMP2 (type 2 AMP) fibres with an enlarged view of one sector at a scale bar corresponding to 10 µm. The surface topography of the fibres appears smooth, and the peptides on the enlarged view appear dotted. It is assumed that the AMPs are embedded within the polymer matrix and also on the surface of the PEO nanofibres.

3.4 | Fourier transform infrared spectroscopy (FTIR) analysis

Figure 5 depicts a characteristic peak corresponding to the PEO observed at 2900 cm^{-1} (methylene group CH 2 molecular stretching)

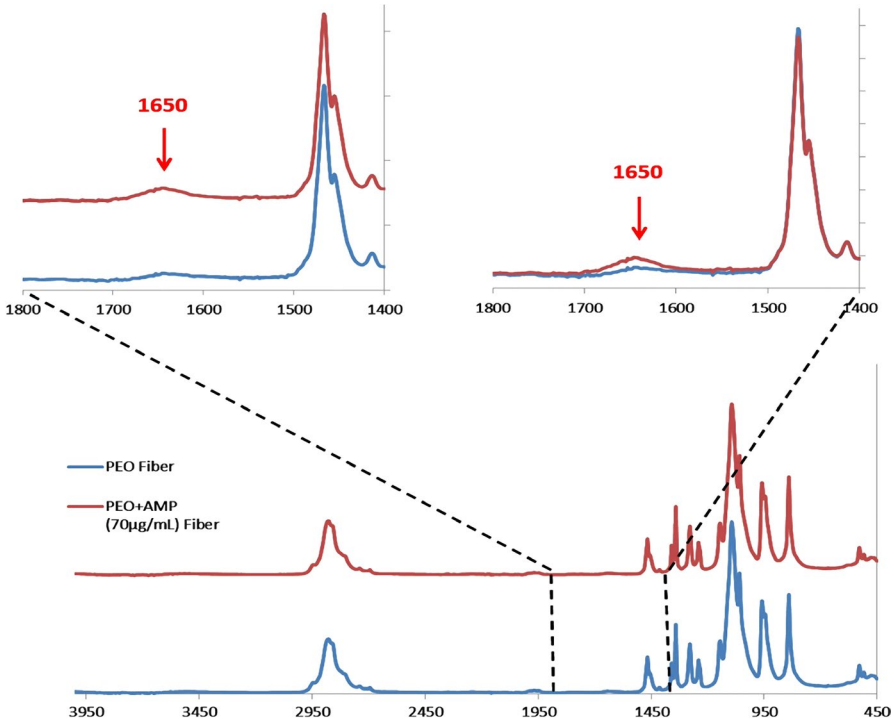

FIGURE 5 FTIR spectra of the nanofibre samples

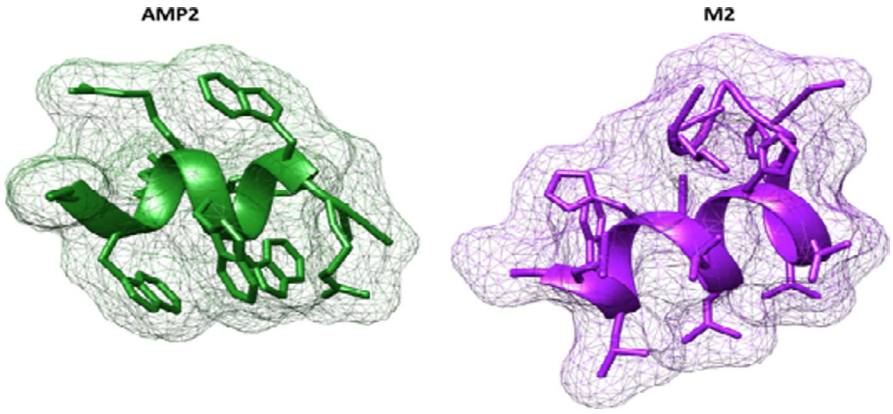

FIGURE 6 Secondary structure models for AMP2 and M2 peptides

TABLE 1 Physical chemical properties of AMP2 and M2 peptides, including the isoelectric point (pI), charge and grand average hydropathy value (GRAVY) determined using the ExPASy ProtParam server

Name	Sequence	#AA	MW	pI	Charge	GRAVY	Hydrophobic Ratio
AMP2	KWKRWWWWR	9	1517.8	12.02	+4	−2.367	55%
GH12-M2	GLLWHLLHHLLHGSGGGK	18	1932.26	8.78	+1	0.133	38%A

The hydrophobic ratio was determined using the APD to calculate and predict tool.

and at 1100 cm^{-1} and 960 cm^{-1} (C O C group stretching) for all of the samples. FTIR results showed that the chemical structure had not changed as a result of M2 integration to fibres. FTIR of the M2 samples integrated with PEO in the two different concentrations did not reveal any additional chemical bonds. Therefore, FTIR peaks of PEO fibre and fibre samples containing M2 are similar. The slight peak

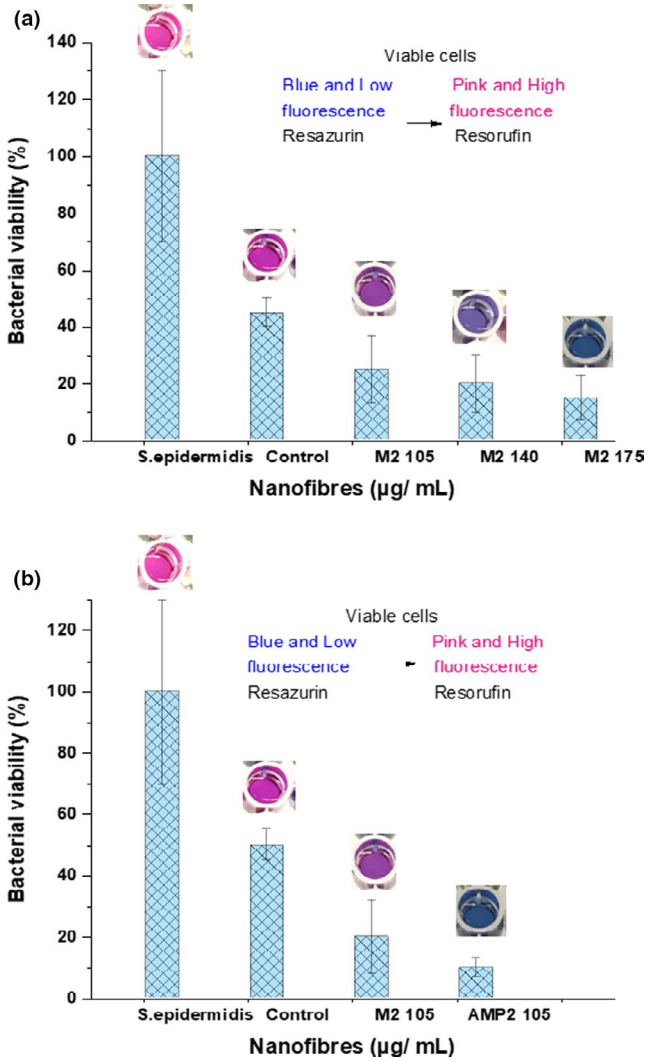

FIGURE 7 (a) Antimicrobial effect of PEO fibres loaded with different concentrations of M2 peptides (type 1 AMP) at 105–175 µg/ml against *Staphylococcus epidermidis* evaluated with AlamarBlue cell viability assay, and (b) Comparison of antimicrobial effect of PEO fibres loaded with M2 and AMP2 peptides (type 1 and type 2 AMPs) at 105 µg/ml against *S. epidermidis*

at 1650 cm^{-1} is assumed to correspond to the addition of the peptide, while retaining the bulk chemical properties of the control PEO fibres.

3.5 | Antimicrobial peptide structures

AMP integrated fibres were produced using M2 (type 1 AMP) and AMP2 (type 2 AMP) peptides. PEP-FOLD 3.5.8 was used to obtain the secondary structure peptide models from the amino acid sequences (Lamiable et al., 2016) (Figure 6). Physical and chemical properties for each of the AMPs were determined using the ExPASy ProtPram server (Gasteiger et al., 2005) (Table 1). The hydrophobic ratio was calculated using the Antimicrobial Peptide Database (APD) Calculate and Predict tool (Wang et al., 2015). Characteristic properties of AMPs include cationic charge, amphipathicity, hydrophobicity and α-helix secondary structure (Koehbach & Craik, 2019). Previously, AMP2 has been linked to a titanium binding domain through an engineered spacer as a chimeric peptide in order to bring antimicrobial function to the titanium medical implants (Yucesoy et al., 2015). Chimeric peptides with incorporated AMP2 demonstrated successful antibacterial function against *S. epidermidis*. However, this AMP has not been previously investigated as an agent incorporated in polymeric nanofibres designed to address infection-related challenges associated with wound healing. It was determined through de novo structure modelling that AMP2 has the α-helix secondary structure frequently observed in other AMPs with strong activity against pathogens such as *S. epidermidis* (Wisdom et al., 2016). Moreover, the cationic charge and moderate hydrophobic ratio support the use of this peptide as an antimicrobial agent suitable for incorporation into polymeric nanofibres. The M2 peptide model shows mostly α-helix secondary structure with a positive charge; however, the hydrophobic ratio is lower than the hydrophobic ratio of AMP2. This could support AMP2 functioning more effectively as an AMP compared to M2 (Wisdom et al., 2020).

3.6 | Bacterial viability

Figure 7a shows the bacterial viability of 105 CFU/ml *S. epidermidis* using the control PEO-nanofibre sample and PEO-M2 nanofibre samples at varying concentrations (105–175 µg/ml). In Figure 7a, the PEO-control samples are not incorporated with any AMPs; it could be observed that approximately 40% of the cells are viable, while using 105 µg/ml PEO-M2 nanofibres, approximately 20% are viable. Figure 7a shows that after increasing the M2 concentration to 175 µg/ml, approximately 10% of *S. epidermidis* are alive. It should also be noted that the release of AMP was almost instantaneous; this is due to using a water-soluble polymer. The results here display a significant bacterial reduction with PEO-M2 nanofibres with increasing concentrations.

Figure 7b shows the bacterial viability of *S. epidermidis* by comparing the PEO-control nanofibre sample, 105 µg/ml PEO-M2 nanofibres, and 105 µg/ml PEO-AMP2 nanofibres. At the same concentration (105 µg/ml), Figure 7b shows a significant reduction in bacterial growth with PEO-AMP2, which shows that there is a stronger antibacterial effect on *S. epidermidis* compared with PEO-M2 nanofibres. From the results shown, it is observed that PEO-AMP2 retains a 10% bacterial viability, whereas PEO-M2 leads to about 20% viability. However, at 175 µg/ml PEO-M2, similar viability was achieved (Figure 7a) compared to that of 105 µg/ml PEO-AMP2. Thus, Figure 7b indicates that the most significant bacterial reduction was obtained at an AMP concentration of 105 µg/ml PEO-AMP2.

4 | CONCLUSIONS AND FUTURE PROSPECTS

Pressurized gyration method was used to produce PEO-nanofibre mesh with AMPs. We incorporated two different AMPs into the PEO

nanofibres at varying concentrations (35 μg/ml–175 μg/ml) to investigate the highest bacterial reduction for *S. epidermidis*, which is a common bacterium associated with wound related complications. The fabricated nanofibres demonstrated a high efficacy against *S. epidermidis*. The assessment of bacterial viability indicated a significant decrease in bacterial population with an increase in the AMP concentration. Both M2 and AMP2 peptides confirmed promising bacterial reduction; however, the greatest bacterial reduction was achieved with 105 μg/ml PEO-AMP2 nanofibres. Loading antibacterial peptides with water-soluble polymers such as PEO is an effective delivery method for the rapid release of antimicrobial ailment into a wound site. Furthermore, using water-based solvent systems also allows more environmentally friendly approaches while also ensuring maximal biocompatibility in open wound scenarios. The work presented here shows that AMPs incorporated into nanofibres are a promising design choice as biological dressings for the next generation of wound healing products. PG has now evolved further to make core-sheath fibres (Mahalingam et al., 2020; Mahalingam et al., 2020). Here the sheath contains a functional material which can be attached to a polymer while the core is a strong polymer. Thus, the AMPs can be in the PEO sheath and this will further enhance our strategy to manufacture wound healing meshes.

REFERENCES

Adam, P., Sasikanth, K., Nama, S., Suresh, S., & Brahmaiah, B. (2013). Nanofibers - A new trend in nano drug delivery. *International Journal of Pharmaceutical Research & Analysis*, *3*, 47–55.

Agarwal, S., Sharma, G., Dang, S., Gupta, S., & Gabrani, R. (2016). Antimicrobial peptides as anti-infectives against Staphylococcus epidermidis. *Medical Principles and Practice*, *25*(4), 301–308. https://doi.org/10.1159/000443479

Alenezi, H., Cam, M. E., & Edirisinghe, M. (2019). Experimental and theoretical investigation of the fluid behavior during polymeric fiber formation with and without pressure. *Applied Physics Reviews*, *6*(4), 041401. https://doi.org/10.1063/1.5110965

Al-Enizi, A. M., Zagho, M. M., & Elzatahry, A. A. (2018). Polymer-based electrospun nanofibers for biomedical applications. *Nanomaterials (Basel, Switzerland)*, *8*(4), 259. https://doi.org/10.3390/nano8040259

Atkin, L., Bućko, Z., Montero, E. C., Cutting, K., Moffatt, C., Probst, A., Romanelli, M., Schultz, G. S., & Tettelbach, W. (2019). Implementing TIMERS: the race against hard-to-heal wounds. *Journal of Wound Care*, *28*(Sup3a), S1–S50. https://doi.org/10.12968/jowc.2019.28.Sup3a.S1

Caló, E., & Khutoryanskiy, V. V. (2015). Biomedical applications of hydrogels: A review of patents and commercial products. *European Polymer Journal*, *65*, 252–267. https://doi.org/10.1016/j.eurpolymj.2014.11.024

Chen, C., Dirican, M., & Zhang, X. W. (2019). *Centrifugal spinning-high rate production of nanofibers*. Elsevier Science Bv.

Chou, S., Wang, J., Shang, L. U., Akhtar, M. U., Wang, Z., Shi, B., Feng, X., & Shan, A. (2019). Short, symmetric-helical peptides have narrow-spectrum activity with low resistance potential and high selectivity. *Biomaterials Science*, *7*(6), 2394–2409. https://doi.org/10.1039/c9bm00044e

Dabiri, G., Damstetter, E., & Phillips, T. (2016). Choosing a wound dressing based on common wound characteristics. *Advances in Wound Care*, *5*(1), 32–41. https://doi.org/10.1089/wound.2014.0586

DeFrates, K. G., Moore, R., Borgesi, J., Lin, G., Mulderig, T., Beachley, V., & Hu, X. (2018). Protein-based fiber materials in medicine: A review. *Nanomaterials (Basel, Switzerland)*, *8*(7), 457. https://doi.org/10.3390/nano8070457

Dreifke, M. B., Jayasuriya, A. A., & Jayasuriya, A. C. (2015). Current wound healing procedures and potential care. *Materials Science & Engineering C-Materials for Biological Applications*, *48*, 651–662. https://doi.org/10.1016/j.msec.2014.12.068

Dumville, J. C., Gray, T. A., Walter, C. J., Sharp, C. A., Page, T., Macefield, R., Blencowe, N., Milne, T. K. G., Reeves, B. C., & Blazeby, J. (2016). Dressings for the prevention of surgical site infection. *Cochrane Database of Systematic Reviews*, *12*(12), CD003091. https://doi.org/10.1002/14651858.CD003091.pub4

Ebenhan, T., Gheysens, O., Kruger, H. G., Zeevaart, J. R., & Sathekge, M. M. (2014). Antimicrobial peptides: Their role as infection-selective tracers for molecular imaging. *Biomed Research International*, *2014*, 1–15. https://doi.org/10.1155/2014/867381

Eming, S. A., Martin, P., & Tomic-Canic, M. (2014). Wound repair and regeneration: Mechanisms, signaling, and translation. *Science Translational Medicine*, *6*(265), 265sr6. https://doi.org/10.1126/scitranslmed.3009337

Eranka Illangakoon, U., Mahalingam, S., Wang, K., Cheong, Y.-K., Canales, E., Ren, G. G., Cloutman-Green, E., Edirisinghe, M., & Ciric, L. (2017). Gyrospun antimicrobial nanoparticle loaded fibrous polymeric filters. *Materials Science & Engineering C-Materials for Biological Applications*, *74*, 315–324. https://doi.org/10.1016/j.msec.2016.12.001

Fjell, C. D., Jenssen, H., Cheung, W. A., Hancock, R. E. W., & Cherkasov, A. (2011). Optimization of antibacterial peptides by genetic algorithms and cheminformatics. *Chemical Biology & Drug Design*, *77*(1), 48–56. https://doi.org/10.1111/j.1747-0285.2010.01044.x

Gasteiger, E., Hoogland, C., Gattiker, A., Duvaud, S. E., Wilkins, M. R., Appel, R. D., & Bairoch, A. (2005). Protein identification and analysis tools on the ExPASy server. In J. M. Walker (Ed.), *The proteomics protocols handbook* (pp. 571–607). Humana Press.

Georgescu, M., Chifiriuc, M. C., Marutescu, L., Gheorghe, I., Lazar, V., Bolocan, A., & Bertesteanu, S. (2017). Bioactive wound dressings for the management of chronic wounds. *Current Organic Chemistry*, *21*(1), 53–63. https://doi.org/10.2174/1385272820666160510171040

Ghomi, E. R., Khalili, S., Khorasani, S. N., Neisiany, R. E., & Ramakrishna, S. (2019). Wound dressings: Current advances and future directions. *Journal of Applied Polymer Science*, *136*(27), 12. https://doi.org/10.1002/app.47738

Gizaw, M., Thompson, J., Faglie, A., Lee, S.-Y., Neuenschwander, P., & Chou, S.-F. (2018). Electrospun fibers as a dressing material for drug and biological agent delivery in wound healing applications. *Bioengineering (Basel, Switzerland)*, *5*(1), 9. https://doi.org/10.3390/bioengineering5010009

Gonzalez, A. C. D. O., Costa, T. F., Andrade, Z. D. A., & Medrado, A. R. A. P. (2016). Wound healing - A literature review. *Anais Brasileiros De Dermatologia*, *91*(5), 614–620. https://doi.org/10.1590/abd1806-4841.20164741

Han, G., & Ceilley, R. (2017). Chronic wound healing: A review of current management and treatments. *Advances in Therapy*, *34*(3), 599–610. https://doi.org/10.1007/s12325-017-0478-y

Hasatsri, S., Pitiratanaworanat, A., Swangwit, S., Boochakul, C., & Tragoonsupachai, C. (2018). Comparison of the morphological and physical properties of different absorbent wound dressings. *Dermatology Research and Practice*, *2018*, 9367034. https://doi.org/10.1155/2018/9367034

Hassiba, A. J., El Zowalaty, M. E., Webster, T. J., Abdullah, A. M., Nasrallah, G. K., Khalil, K. A., & Elzatahry, A. A. (2017). Synthesis, characterization, and antimicrobial properties of novel double layer nanocomposite electrospun fibers for wound dressing applications.

International Journal of Nanomedicine, *12*, 2205–2213. https://doi.org/10.2147/ijn.S123417

Heseltine, P. L., Ahmed, J., & Edirisinghe, M. (2018). Developments in pressurized gyration for the mass production of polymeric fibers. *Macromolecular Materials and Engineering*, *303*(9), 1800218. https://doi.org/10.1002/mame.201800218

Jalili Tabaii, M., & Emtiazi, G. (2018). Transparent nontoxic antibacterial wound dressing based on silver nano particle/bacterial cellulose nano composite synthesized in the presence of tripolyphosphate. *Journal of Drug Delivery Science and Technology*, *44*, 244–253. https://doi.org/10.1016/j.jddst.2017.12.019

Joo, H. S., Fu, C. I., & Otto, M. (2016). Bacterial strategies of resistance to antimicrobial peptides. *Philosophical Transactions of the Royal Society B: Biological Sciences*, *371*(1695), 20150292. https://doi.org/10.1098/rstb.2015.0292

Jun, I., Han, H.-S., Edwards, J. R., & Jeon, H. (2018). Electrospun fibrous scaffolds for tissue engineering: Viewpoints on architecture and fabrication. *International Journal of Molecular Sciences*, *19*(3), 745. https://doi.org/10.3390/ijms19030745

Kamoun, E. A., Kenawy, E.-R.-S., & Chen, X. (2017). A review on polymeric hydrogel membranes for wound dressing applications: PVA-based hydrogel dressings. *Journal of Advanced Research*, *8*(3), 217–233. https://doi.org/10.1016/j.jare.2017.01.005

Kenry, C. T. L. (2017). Nanofiber technology: current status and emerging developments. *Progress in Polymer Science*, *70*, 1–17. https://doi.org/10.1016/j.progpolymsci.2017.03.002

Koehbach, J., & Craik, D. J. (2019). The vast structural diversity of antimicrobial peptides. *Trends in Pharmacological Sciences*, *40*(7), 517–528. https://doi.org/10.1016/j.tips.2019.04.012

Kumar, P., Kizhakkedathu, J. N., & Straus, S. K. (2018). Antimicrobial peptides: Diversity, mechanism of action and strategies to improve the activity and biocompatibility in vivo. *Biomolecules*, *8*(1), 24. https://doi.org/10.3390/biom8010004

Lamiable, A., Thévenet, P., Rey, J., Vavrusa, M., Derreumaux, P., & Tufféry, P. (2016). PEP-FOLD3: faster de novo structure prediction for linear peptides in solution and in complex. *Nucleic Acids Research*, *44*(W1), W449–W454. https://doi.org/10.1093/nar/gkw329

Landén, N. X., Li, D., & Ståhle, M. (2016). Transition from inflammation to proliferation: a critical step during wound healing. *Cellular and Molecular Life Sciences*, *73*(20), 3861–3885. https://doi.org/10.1007/s00018-016-2268-0

Lasocka, I., Jastrzębska, E., Szulc-Dąbrowska, L., Skibniewski, M., Pasternak, I., Kalbacova, M. H., & Skibniewska, E. M. (2019). The effects of graphene and mesenchymal stem cells in cutaneous wound healing and their putative action mechanism. *International Journal of Nanomedicine*, *14*, 2281–2299. https://doi.org/10.2147/IJN.S190928

Lee, H.-J., Lee, S., Uthaman, S., Thomas, R., Hyun, H., Jeong, Y., Cho, C.-S., & Park, I.-K. (2015). Biomedical applications of magnetically functionalized organic/inorganic hybrid nanofibers. *International Journal of Molecular Sciences*, *16*(6), 13661–13677. https://doi.org/10.3390/ijms160613661

Lei, J., Sun, L., Huang, S., Zhu, C., Li, P., He, J., & He, Q. (2019). The antimicrobial peptides and their potential clinical applications. *American Journal of Translational Research*, *11*(7), 3919–3931.

Leng, G., Zhang, X., Shi, T., Chen, G., Wu, X., Liu, Y., Fang, M., Min, X., & Huang, Z. (2019). Preparation and properties of polystyrene/silica fibres flexible thermal insulation materials by centrifugal spinning. *Polymer*, *185*, 8. https://doi.org/10.1016/j.polymer.2019.121964

Liu, Y., Zhou, S., Gao, Y., & Zhai, Y. (2019). Electrospun nanofibers as a wound dressing for treating diabetic foot ulcer. *Asian Journal of Pharmaceutical Sciences*, *14*(2), 130–143. https://doi.org/10.1016/j.ajps.2018.04.004

Lombardi, L., Falanga, A., Del Genio, V., & Galdiero, S. (2019). A new hope: Self-assembling peptides with antimicrobial activity. *Pharmaceutics*, *11*(4), 17. https://doi.org/10.3390/pharmaceutics11040166

Mahalingam, S., Huo, S. G., Homer-Vanniasinkam, S., & Edirisinghe, M. (2020). Generation of core-sheath polymer nanofibers by pressurised gyration. *Polymers*, *12*(8), 13. https://doi.org/10.3390/polym12081709

Mahalingam, S., Matharu, R., Homer-Vanniasinkam, S., & Edirisinghe, M. (2020). Current methodologies and approaches for the formation of core–sheath polymer fibers for biomedical applications. *Applied Physics Reviews*, *7*(4), 041302. https://doi.org/10.1063/5.0008310

Mahlapuu, M., Håkansson, J., Ringstad, L., & Björn, C. (2016). Antimicrobial peptides: An emerging category of therapeutic agents. *Frontiers in Cellular and Infection Microbiology*, *6*, 194. https://doi.org/10.3389/fcimb.2016.00194

Matharu, R. K., Porwal, H., Ciric, L., & Edirisinghe, M. (2018). The effect of graphene-poly(methyl methacrylate) fibres on microbial growth. *Interface Focus*, *8*(3), 9. https://doi.org/10.1098/rsfs.2017.0058

Miguel, S. P., Sequeira, R. S., Moreira, A. F., Cabral, C. S. D., Mendonca, A. G., Ferreira, P., & Correia, I. J. (2019). An overview of electrospun membranes loaded with bioactive molecules for improving the wound healing process. *European Journal of Pharmaceutics and Biopharmaceutics*, *139*, 1–22. https://doi.org/10.1016/j.ejpb.2019.03.010

Mir, M., Ali, M. N., Barakullah, A., Gulzar, A., Arshad, M., Fatima, S., & Asad, M. (2018). Synthetic polymeric biomaterials for wound healing: A review. *Progress in Biomaterials*, *7*(1), 1–21. https://doi.org/10.1007/s40204-018-0083-4

Morais, D. S., Guedes, R. M., & Lopes, M. A. (2016). Antimicrobial approaches for textiles: From research to market. *Materials*, *9*(6), 21. https://doi.org/10.3390/ma9060498

Negut, I., Grumezescu, V., & Grumezescu, A. M. (2018). Treatment strategies for infected wounds. *Molecules (Basel, Switzerland)*, *23*(9), 2392. https://doi.org/10.3390/molecules23092392

Nguyen, A. V., & Soulika, A. M. (2019). The dynamics of the skin's immune system. *International Journal of Molecular Sciences*, *20*(8), 1811. https://doi.org/10.3390/ijms20081811

Nguyen, L. T. H., Chen, S., Elumalai, N. K., Prabhakaran, M. P., Zong, Y., Vijila, C., Allakhverdiev, S. I., & Ramakrishna, S. (2013). Biological, chemical, and electronic applications of nanofibers. *Macromolecular Materials and Engineering*, *298*(8), 822–867. https://doi.org/10.1002/mame.201200143

Pilehvar-Soltanahmadi, Y., Dadashpour, M., Mohajeri, A., Fattahi, A., Sheervalilou, R., & Zarghami, N. (2017). An overview on application of natural substances incorporated with electrospun nanofibrous scaffolds to development of innovative wound dressings. *Mini-Reviews in Medicinal Chemistry*, *18*(5), 414–427. https://doi.org/10.2174/1389557517666170308112147

Rahimnejad, M., Derakhshanfar, S., & Zhong, W. (2017). Biomaterials and tissue engineering for scar management in wound care. *Burns & Trauma*, *5*, 4. https://doi.org/10.1186/s41038-017-0069-9

Rezk, A. I., Rajan Unnithan, A., Hee Park, C., & Sang Kim, C. (2018). Rational design of bone extracellular matrix mimicking tri-layered composite nanofibers for bone tissue regeneration. *Chemical Engineering Journal*, *350*, 812–823. https://doi.org/10.1016/j.cej.2018.05.185

Saghazadeh, S., Rinoldi, C., Schot, M., Kashaf, S. S., Sharifi, F., Jalilian, E., Nuutila, K., Giatsidis, G., Mostafalu, P., Derakhshandeh, H., Yue, K., Swieszkowski, W., Memic, A., Tamayol, A., & Khademhosseini, A. (2018). Drug delivery systems and materials for wound healing applications. *Advanced Drug Delivery Reviews*, *127*, 138–166. https://doi.org/10.1016/j.addr.2018.04.008

Shahriar, S. M. S., Mondal, J., Hasan, M. N., Revuri, V., Lee, D. Y., & Lee, Y.-K. (2019). Electrospinning Nanofibers for Therapeutics Delivery. *Nanomaterials (Basel, Switzerland)*, *9*(4), 532. https://doi.org/10.3390/nano9040532

Sharma, J., Lizu, M., Stewart, M., Zygula, K., Lu, Y., Chauhan, R., Yan, X. R., Guo, Z. H., Wujcik, E. K., & Wei, S. Y. (2015). Multifunctional Nanofibers towards Active Biomedical Therapeutics. *Polymers*, *7*(2), 186–219. https://doi.org/10.3390/polym7020186

Shen, Y., Maupetit, J., Derreumaux, P., & Tufféry, P. (2014). Improved PEP-FOLD approach for peptide and miniprotein structure prediction. *Journal of Chemical Theory and Computation*, *10*(10), 4745–4758. https://doi.org/10.1021/ct500592m

Simoes, D., Miguel, S. P., Ribeiro, M. P., Coutinho, P., Mendonca, A. G., & Correia, I. J. (2018). Recent advances on antimicrobial wound dressing: A review. *European Journal of Pharmaceutics and Biopharmaceutics*, *127*, 130–141. https://doi.org/10.1016/j.ejpb.2018.02.022

Sood, A., Granick, M. S., & Tomaselli, N. L. (2014). Wound dressings and comparative effectiveness data. *Advances in Wound Care*, *3*(8), 511–529. https://doi.org/10.1089/wound.2012.0401

Stone, R. II, Natesan, S., Kowalczewski, C. J., Mangum, L. H., Clay, N. E., Clohessy, R. M., Carlsson, A. H., Tassin, D. H., Chan, R. K., Rizzo, J. A., & Christy, R. J. (2018). Advancements in regenerative strategies through the continuum of burn care. *Frontiers in Pharmacology*, *9*, 672. https://doi.org/10.3389/fphar.2018.00672

Sun, Y., Cheng, S., Lu, W., Wang, Y., Zhang, P., & Yao, Q. (2019). Electrospun fibers and their application in drug controlled release, biological dressings, tissue repair, and enzyme immobilization. *RSC Advances*, *9*(44), 25712–25729. https://doi.org/10.1039/C9RA05012D

Takeo, M., Lee, W., & Ito, M. (2015). Wound healing and skin regeneration. *Cold Spring Harbor Perspectives in Medicine*, *5*(1), a023267. https://doi.org/10.1101/cshperspect.a023267

Tesauro, D., Accardo, A., Diaferia, C., Milano, V., Guillon, J., Ronga, L., & Rossi, F. (2019). Peptide-based drug-delivery systems in biotechnological applications: Recent advances and perspectives. *Molecules (Basel, Switzerland)*, *24*(2), 27. https://doi.org/10.3390/molecules24020351

Thakkar, S., & Misra, M. (2017). Electrospun polymeric nanofibers: New horizons in drug delivery. *European Journal of Pharmaceutical Sciences*, *107*, 148–167. https://doi.org/10.1016/j.ejps.2017.07.001

Troncoso, O. P., & Torres, F. G. (2020). Non-conventional starch nanoparticles for drug delivery applications. *Medical Devices & Sensors*, e10111. https://doi.org/10.1002/mds3.10111

Uzun, M. (2018). A review of wound management materials. *Journal of Textile Engineering & Fashion Technology*, *4*(1), 00121. https://doi.org/10.15406/jteft.2018.04.00121

Wang, G., Li, X., & Wang, Z. (2015). APD3: the antimicrobial peptide database as a tool for research and education. *Nucleic Acids Research*, *44*(D1), D1087–D1093. https://doi.org/10.1093/nar/gkv1278

Wang, Y., Zeng, Y., Wang, Y., Li, H., Yu, S., Jiang, W., & Zhang, L. (2019). Antimicrobial peptide GH12 targets Streptococcus mutans to arrest caries development in rats. *Journal of Oral Microbiology*, *11*(1), 1549921. https://doi.org/10.1080/20002297.2018.1549921

Wisdom, C., VanOosten, S. K., Boone, K. W., Khvostenko, D., Arnold, P. M., Snead, M. L., & Tamerler, C. (2016). Controlling the biomimetic implant interface: Modulating antimicrobial activity by spacer design. *Journal of Molecular and Engineering Materials*, *4*(1), 1640005. https://doi.org/10.1142/S2251237316400050

Wisdom, E. C., Zhou, Y., Chen, C., Tamerler, C., & Snead, M. L. (2020). Mitigation of peri-implantitis by rational design of bifunctional peptides with antimicrobial properties. *ACS Biomaterials Science & Engineering*, *6*(5), 2682–2695. https://doi.org/10.1021/acsbiomaterials.9b01213

Xie, S.-X., Boone, K., VanOosten, S. K., Yuca, E., Song, L., Ge, X., Ye, Q., Spencer, P., & Tamerler, C. (2019). Peptide mediated antimicrobial dental adhesive system. *Applied Sciences*, *9*(3), 557. https://doi.org/10.3390/app9030557

Xue, J., Wu, T., Dai, Y., & Xia, Y. (2019). Electrospinning and electrospun nanofibers: Methods, materials, and applications. *Chemical Reviews*, *119*(8), 5298–5415. https://doi.org/10.1021/acs.chemrev.8b00593

Yang, Z., Zheng, J., Chan, C.-F., Wong, I. L. K., Heater, B. S., Chow, L. M. C., Lee, M. M. M., & Chan, M. K. (2019). Targeted delivery of antimicrobial peptide by Cry protein crystal to treat intramacrophage infection. *Biomaterials*, *217*, 14. https://doi.org/10.1016/j.biomaterials.2019.119286

Yazici, H., O'Neill, M. B., Kacar, T., Wilson, B. R., Oren, E. E., Sarikaya, M., & Tamerler, C. (2016). Engineered chimeric peptides as antimicrobial surface coating agents toward infection-free implants. *ACS Applied Materials and Interfaces*, *8*(8), 5070–5081. https://doi.org/10.1021/acsami.5b03697

Ye, K., Kuang, H., You, Z., Morsi, Y., & Mo, X. (2019). Electrospun nanofibers for tissue engineering with drug loading and release. *Pharmaceutics*, *11*(4), 182. https://doi.org/10.3390/pharmaceutics11040182

Yin, L. M., Yuvienco, C., & Montclare, J. K. (2017). Protein based therapeutic delivery agents: Contemporary developments and challenges. *Biomaterials*, *134*, 91–116. https://doi.org/10.1016/j.biomaterials.2017.04.036

Yucesoy, D. T., Hnilova, M., Boone, K., Arnold, P. M., Snead, M. L., & Tamerler, C. (2015). Chimeric peptides as implant functionalization agents for titanium alloy implants with antimicrobial properties. *JOM Journal of the Minerals Metals and Materials Society*, *67*(4), 754–766. https://doi.org/10.1007/s11837-015-1350-7

Zharkova, M. S., Orlov, D. S., Golubeva, O. Y., Chakchir, O. B., Eliseev, I. E., Grinchuk, T. M., & Shamova, O. V. (2019). Application of antimicrobial peptides of the innate immune system in combination with conventional antibiotics-a novel way to combat antibiotic resistance? *Frontiers in Cellular and Infection Microbiology*, *9*, 128. https://doi.org/10.3389/fcimb.2019.00128

Zhen, J.-B., Zhao, M.-H., Ge, Y., Liu, Y. A., Xu, L.-W., Chen, C., Gong, Y.-K., & Yang, K.-W. (2019). Construction, mechanism, and antibacterial resistance insight into polypeptide-based nanoparticles. *Biomaterials Science*, *7*(10), 4142–4152. https://doi.org/10.1039/c9bm01050e

How to cite this article: Afshar A, Yuca E, Wisdom C, et al. Next-generation Antimicrobial Peptides (AMPs) incorporated nanofibre wound dressings. *Med Devices Sens*. 2021;4:e10144. https://doi.org/10.1002/mds3.10144